Integrated 3D motion analysis with functional magnetic resonance neuroimaging to identify neural correlates of lower extremity movement

Manish Anand[1,5], **Jed A. Diekfuss**[1,5,6], **Alexis B. Slutsky-Ganesh**[2], **Dustin R. Grooms**[3,4], **Scott Bonnette**[1], **Kim D. Barber Foss**[1,5], **Christopher A. DiCesare**[1], **Jennifer L. Hunnicutt**[6], **Gregory D. Myer**[1,5,6,7,8,9]

[1]The SPORT Center, Division of Sports Medicine, Cincinnati Children's Hospital Medical Center, Cincinnati, OH, USA

[2]Department of Kinesiology, University of North Carolina at Greensboro, Greensboro, NC, USA

[3]Ohio Musculoskeletal & Neurological Institute, Ohio University, Athens, OH, USA

[4]Division of Athletic Training, School of Applied Health Sciences and Wellness, College of Health Sciences and Professions, Ohio University, Athens, OH, USA

[5]Sport Performance And Research Center, Flowery Branch, GA, USA

[6]Department of Orthopaedics, Emory School of Medicine, Emory University, Atlanta, GA, USA

[7]Emory Sports Medicine Center, Atlanta, GA, USA

[8]Department of Pediatrics and Orthopaedic Surgery, University of Cincinnati, Cincinnati, OH, USA

[9]The Micheli Center for Sports Injury Prevention, Waltham, MA, USA

Abstract

Background: To better understand the neural drivers of aberrant motor control, methods are needed to identify whole brain neural correlates of isolated joints during multi-joint lower-

extremity coordinated movements. This investigation aimed to identify the neural correlates of knee kinematics during a unilateral leg press task.

New Method: The current study utilized an MRI-compatible motion capture system in conjunction with a lower extremity unilateral leg press task during fMRI. Knee joint kinematics and brain activity were collected concurrently and averaged range of motion were modeled as covariates to determine the neural substrates of knee out-of-plane (frontal) and in-plane (sagittal) range of motion.

Results: Increased out-of-plane (frontal) range of motion was associated with altered brain activity in regions important for attention, sensorimotor control, and sensorimotor integration ($z > 3.1$, $p < .05$), but no such correlates were found with in-plane (sagittal) range of motion ($z > 3.1$, $p > .05$).

Comparison with Existing Method(s): Previous studies have either presented overall brain activation only, or utilized biomechanical data collected outside MRI in a standard biomechanics lab for identifying single-joint neural correlates.

Conclusions: The study shows promise for the MRI-compatible system to capture lower-extremity biomechanical data collected concurrently during fMRI, and the present data identified potentially unique neural drivers of aberrant biomechanics.

Future research can adopt these methods for patient populations with CNS-related movement disorders to identify single-joint kinematic neural correlates that may adjunctively supplement brain-body therapeutic approaches.

1. Introduction

Discovery of the brain activity associated with lower extremity multi-joint motor coordination is important to better understand injuries or pathologies that affect mobility (e.g., knee osteoarthritis, patellofemoral pain, chronic low back pain) (Needle et al., 2017; Neto et al., 2019; Pelletier et al., 2015; Silfies et al., 2017; Te et al., 2017). For instance, musculoskeletal injuries have typically been considered structural joint problems, but recent investigations into lower extremity motor control have revealed alterations in brain function are associated with many joint and related ligament injuries (Needle et al., 2017; Neto et al., 2019). Of these, knee anterior cruciate ligament (ACL) injury is particularly prevalent in physically-active populations and (Abram et al., 2020), despite surgical reconstruction and extensive rehabilitation, is often associated with long-term reduced function (Lohmander et al., 2007). Two common biomechanical risk factors for ACL injury are increased knee valgus in the frontal plane and decreased knee flexion in the sagittal plane during dynamic multi-joint coordinated movements such as landing and change of direction maneuvers (a 'stiff' movement strategy that strains the ACL) (Dingenen et al., 2015; Havens & Sigward, 2015; Hewett et al., 2005; Paterno et al., 2010). As the majority of ACL injury events are noncontact, as in occurring secondary to motor 'coordination' errors that regulate knee position and not direct blows or player contact, central nervous system (CNS) processing

of knee position has been implicated to play a role (Bonnette et al., 2020; Diekfuss, Grooms, Nissen, et al., 2019; Diekfuss, Grooms, Yuan, et al., 2019; Grooms et al., 2015; Swanik, 2015). Accordingly, preliminary methods have emerged to discover how the CNS contributes to knee injury-risk movement mechanics to support the development of combined brain and body therapeutics for those with and without movement disorders (Armijo-Olivo, 2018; Bonnette et al., 2020; Diekfuss, Grooms, Bonnette, et al., 2020; Grooms et al., 2018; Silfies et al., 2017).

Prior studies have utilized modalities with either high temporal resolution (e.g. Extracranial electroencephalography [EEG], functional near infrared spectroscopy [fNIRS]) or high spatial resolution (e.g. functional magnetic resonance imaging [fMRI]) to elucidate different aspects of movement neural correlates. EEG has shown promise in light of its portability and relatively high temporal resolution for mobile brain imaging (Malcolm et al., 2015; Seeber et al., 2014, 2015; Wagner et al., 2019). Indeed, numerous studies have successfully acquired electrocortical activity and managed head motion artifact with EEG during gross motor control tasks including static balance, dynamic balance using movable platforms, gait, running, and other locomotion-related movements (Edwards et al., 2018; Gebel et al., 2020; Gwin & Ferris, 2012; Oliveira et al., 2016, 2017; Peterson & Ferris, 2018). Despite its high temporal resolution, EEG has poor spatial resolution, thus precluding precise measurement of the *subcortical* neural activity (e.g., the cerebellum, basal ganglia) critically important for nearly all tasks that require movement of the lower extremity (Fukuyama et al., 1997; Grooms et al., 2019; la Fougère et al., 2010). Likewise, other modalities including fNIRS have enhanced our understanding of the neural correlates of movement (Suzuki et al., 2008; Vitorio et al., 2017), but also have limited whole brain spatial resolution, warranting the use of fMRI to localize both cortical and subcortical neural activity for lower extremity motor coordination. For instance, emergent fMRI studies have demonstrated the unique involvement of both cortical and subcortical brain regions during knee flexion and extension movements in patients following knee ligament injury (Criss et al., 2020; Grooms et al., 2015, 2017).

Prior work has employed MRI-safe experimental setups to measure brain activity during lower-extremity tasks including ankle plantarflexion and dorsiflexion (Dobkin et al., 2004; MacIntosh et al., 2004), knee flexion and extension (Criss et al., 2020; Grooms et al., 2015, 2017; Kapreli et al., 2009), cycling (Mehta et al., 2009), combined ankle, knee and hip flexion and extension against external resistance (i.e., a leg press) (Grooms et al., 2018, 2019), and active and passive movements in response to externally simulated stepping (Jaeger et al., 2014, 2015; Marchal-Crespo et al., 2017). However, these paradigms typically examine brain activity of the *entire* lower-extremity multi-joint movement, without isolating the relative influence of *single* joints on neural activity as they move in and out of plane. Reasonably, inter- and intra-subject, single-joint in- and out-of-plane movement variability could distinguish unique neural activity relative to individual motor coordination strategies for complex movement. A logical progression to overcome prior study limitations would be to integrate MRI-compatible methods capable of quantifying single-joint kinematics during multi-joint lower-extremity movements. Therefore, the purpose of this work was to identify both whole brain neural activity elicited during a multi-joint lower extremity leg press task, and the distinct, single-joint brain activity associated with knee sagittal

and frontal plane biomechanics during this movement (in- and out-of-plane kinematics, respectively). To the best of our knowledge, prior literature utilizing multi-planar lower extremity fMRI paradigms have not quantified in- and out-of-plane knee kinematics to isolate how variability in these biomechanical data may uniquely contribute to brain activity.

2.   Methods

2.1.   Participants

Seventeen healthy right leg dominant (self-reported) female soccer and basketball players from local high schools (mean age 14.5±1.4 years; mean height 168.1 ± 6.9 cm; mean weight 62.4 ± 19.5 kg) enrolled in this neuroimaging study. The study was completed in a single visit and all participants and parent/legal guardian signed written informed assent and consent prior to completing MRI screening. The study was approved by the institutional review board at Cincinnati Children's Hospital Medical Center.

2.2.   Procedure

As shown in Figure 1, we adopted an fMRI paradigm consisting of unilateral closed kinetic chain ankle, knee, and hip movement against resistance that reliably reproduces sensorimotor brain activation with minimal head motion artifact (Grooms et al., 2018, 2019). As shown in Figure 2, we utilized an MRI-compatible Metria high field Moiré phase tracking (MPT) motion capture system (Metria Innovation Inc., Wisconsin, USA) for concurrent measurement of lower-extremity biomechanics (Anand, Diekfuss, Bonnette, et al., 2020). For the present study, the camera was installed on a ball pivot above the MRI bore at ~120cm above the table and its position could be adjusted parallel to the bore axis to accommodate subjects of different heights. As seen in Figure 1, Velcro straps affixed with custom motion tracking markers were secured to the participant's thigh and lower leg during fMRI for quantifying multi-planar knee motion (described in section 2.3).

The MRI-compatible leg press apparatus (Figure 1) has a pair of independent, horizontally sliding foot pedals. The participant's feet were strapped to these pedals and an elastic resistance tube (manufacturer rated peak force ~9.1 kgs) was anchored at three points on the lateral side of both legs and in the center of the leg press apparatus. The anchor points were approximately midway between the hips and knees, and the two parts of the resistance tube were looped around the pedals such that when the pedals were pushed, the tubes stretched and provided resistance against extension at the hip, knee, and ankle. Participants were asked to lay supine on the MRI table with their head inside an MRI coil while wearing headphones to hear auditory cues. Their upper body was secured using a combination of four straps across their torso and pelvis. A pair of handles were available to brace against and provide rotational stability. Participants completed four blocks of 30 seconds of unilateral (right leg) ankle, knee, and hip flexion and extension movements interlaced with 30 seconds of rest in between each movement block. The left leg remained still and fully extended throughout data capture. Participants were provided with visual cues at the start and stop of the movement blocks, coupled with a metronome beat at 1.2 Hz for standardizing pace during the movement blocks. To minimize potential for head movement, participants were trained on the entire experimental protocol prior to performing the data

collection. The training session started with the participant watching a video of the leg press task, followed by performing the task to completion in a mock setup. Participants received the visual and auditory prompts and a researcher provided feedback on head motion and expected range of motion to standardize movements (Grooms et al., 2019).

2.3. Biomechanics Data Acquisition and Analysis

The MRI-compatible motion analysis system was previously validated against a 44 camera standard motion capture system in a biomechanics lab for kinematic accuracy of lower extremity movements, reliably acquiring simultaneous data from four markers simultaneously (Anand, Diekfuss, Bonnette, et al., 2020). Each marker consists of characteristic coordinate axes used to define the orientation of the marker during movement. The MRI-compatible markers were placed on both thighs and shins of the subjects as seen in Figure 1. The markers were oriented such that the x-axis of the marker was aligned along the long axis (z-axis) of the limb segment (Grood & Suntay, 1983) and the marker was aligned parallel to the frontal plane of the segment similar to a previous study using a similar motion capture system (Weinhandl et al., 2010). The long axis of a limb segment was approximated by lines connecting the joint centers in the frontal plane, which were measured while the participant lay supine. As a result, the marker axes were aligned with the segment coordinates similar to standard biomechanics practice (Umberger & Caldwell, 2014). The system transmitted data corresponding to each frame and each marker as a UDP packet which was captured on a data collection computer using customized software developed in MATLAB (2018a) (MathWorks, Natick, Massachusetts, USA).

The camera captured the location of the origin of the marker axes and the orientation of each marker (in quaternions) in the camera coordinate system. The system captured the data at 85 Hz which was then processed using custom software developed in MATLAB where data was filtered using a low pass 12 Hz 4th order Butterworth filter.

We focused on average knee range of motion (ROM) kinematics during the move blocks due to these variables' relationship to knee ACL injury. Specifically, high frontal ROM (i.e., excessive valgus/varus or abduction/adduction) and low sagittal ROM (reduced flexion/stiffness) during a closed kinetic chain exercise can stress the ACL and is considered high-risk for ACL injury (Hewett et al., 2005). For this study, knee joint angles were calculated by transforming the shin coordinate system to the thigh coordinate system (Umberger & Caldwell, 2014) and ROM variables in both the sagittal and frontal planes were determined by calculating the difference between the maximum and the minimum angle for each cycle. The ROMs of each cycle were averaged to create the mean ROM of the movement block, which was subsequently averaged over the four blocks for each plane. A sample of data captured for one movement block for a representative subject is shown in Fig. 3 alongwith how ROM for each cycle was determined.

2.4. Neuroimaging Data Acquisition and Analysis

MR scanning was conducted on a Philips 3T Ingenia scanner (Philips Medical Systems, Best, Netherlands) equipped with a 32 channel, phased-array head coil. Congruent with previously employed acquisition methodology (Grooms et al., 2019), an MPRAGE sequence

was used to acquire high resolution 3D T1-weighted images with the following parameters: TR = 8.1 ms, TE = 3.7 ms; field of view = 256 × 256 mm; matrix = 256 × 256; in-plane resolution = 1 × 1 mm; slice thickness = 1 × 1 mm; number of slices = 180. The functional MRI acquisition included 135 whole-brain gradient echo-planar scans with the following parameters: TR = 2000 milliseconds; TE = 35 milliseconds; field of view = 240 × 240 mm; slice thickness = 5 mm; voxel size=3.75 mm x 3.75 mm (Grooms et al., 2019).

fMRI data processing included three steps completed with FMRIB's Software Library (FSL; www.fmrib.ox.ac.uk/fsl). The first step was preprocessing and included robust brain extraction (Smith, 2002), motion correction using MCFLIRT (Jenkinson et al., 2002), ascending slice timing correction, spatial smoothing with a gaussian kernel of 6.0 mm full-width-half-max (FWHM), and multiplicative mean intensity normalization of the volume at each timepoint. Functional images were linearly registered to the high resolution 3D T1-weighted structural images with FLIRT (Jenkinson et al., 2002; Jenkinson & Smith, 2001) and further refined with non-linear registration from high resolution structural images to standard space(T1 2mm brain) (Andersson et al., 2010a, 2010b). Despite some participants displaying task-correlated head motion, no participants were excluded to this point as the second step was meant to improve the usability of data with regard to head motion. Specifically, the second step included use of independent component analysis for automated removal of motion artifacts (ICA-AROMA) (Pruim et al., 2015). ICA-AROMA uses FSL's melodic tool to identify and remove motion related components. Percent of components removed was calculated for each participant. In previous literature, ICA-based removal of artifact from standard 3 Tesla resting-state fMRI sequences has ranged from 70–88% (Griffanti et al., 2014; Rummel et al., 2013), with the removed components being small in size, but high in number, and reflective of motion and physiological artifact. ICA-AROMA is focused on head motion only, which may reduce the amount of noise artifacts removed from the data. Removal of components from the current study's task-based fMRI data ranged from 28.2% – 52.2% (M=42.0%, SD=5.5%), which is similar to previous blocked-design findings (Tohka et al., 2008). Of note, this was not removal of 28.2% – 52.2% of the subjects or data, but removal of that volume of components secondary to their identification to be head motion artifact associated noise. Processing of data with ICA-AROMA and inspection of components and first-level results were completed using INFOBAR (Anand, Diekfuss, Slutsky-ganesh, et al., 2020), the Interface for Batch processing data using ICA-AROMA. Supported by INFOBAR's data visualization features, neuroimaging data was deemed usable for 16 of the 17 participants, as determined by three authors with over 20 years of combined experience analyzing movement-related fMRI data (Authors 2, 3, & 4). 'Usable' was operationally defined as the BOLD signal data having sufficient model fit, with dissociable baseline (i.e., rest) and task (i.e., move) blocks, a stable baseline, and low relative head motion <0.30 mm. Absolute and relative head motion ranged from 0.16mm-1.08mm (M=0.42, SD=0.45) and 0.04–0.26mm (M=0.11, SD=0.07) respectively. Following ICA-AROMA, preprocessing was completed with a third step of subjecting images to a high pass filter (cutoff=100seconds) and completing registration congruent with step one.

First-level, whole-brain analyses were then completed in FSL's fMRI Expert Analysis Tool (FEAT). Time series analyses were carried out using FILM with local autocorrelation

correction (Woolrich et al., 2001) employing a 30 second block design (30 seconds on/30 seconds off), and a cluster-wise threshold of $Z > 3.1$ and $p < .05$. Task performance relative to the model fit was inspected for each participant. One participant was excluded from further analysis due to poor model fit, resulting in 16 participants for higher-level analyses.

Higher level analyses included a one-sample t-test (move > rest) to determine task-elicited activation and the addition of two ROM biomechanics variables as covariates, entered in separate models, to assess their potential unique relationship with brain activity in both directions (positive and negative associations). Specifically, mean knee range of motion in both the frontal and sagittal plane were demeaned and used as covariates. All higher-level analyses were computed over the entire brain with a voxel-wise covariate for gray matter and a cluster-wise threshold of $Z > 3.1$ and $p < .05$.

3.   Results

3.1.   Knee biomechanics

The group mean angle for knee frontal ROM angle was 2.5° ($SD = 1.2°$). The group mean angle for sagittal knee ROM was 11.4° ($SD = 3.4°$).

3.2.   Overall Brain Activity

During the leg press task, there was increased activity (relative to rest) in a cluster (n voxels = 4269) extending over the supplementary motor cortex, the precentral gyrus, and postcentral gyrus ($p < .001$). During the leg press task, there was also increased activity in bilateral clusters extending from the parietal operculum cortex to the planum temporale (Left: $p < .001$, Right: $p = .001$), from the insula to the central opercular cortex (Left: $p = .013$), Right: $p = .034$), and in the cerebellum right lobules I-IV (p<.001). Results are shown in Figure 4 and Table 1.

3.3.   Correlates with Biomechanics Data

As presented in Figure 5 and corresponding details in Table 2, greater frontal range of motion during the leg press task was associated with increased activation (relative to rest) in the posterior cingulate (extends into precuneus; large cluster ($p < .001$), the precuneus ($p = .040$), cerebellum left V/I-IV ($p < .001$), bilateral parahippocampus/temporal fusiform gyrus (Left: $p < .001$, Right: $p = .007$), left pallidum ($p < .001$), left cerebellum VIIIa ($p = .005$), cerebellum right crus I ($p = .008$), and the left middle frontal gyrus ($p = .022$). Furthermore, greater frontal range of motion was associated with reduced activation (relative to rest) in clusters within the frontal pole/superior frontal gyrus ($p < .001$), planum polare/insula/pallidum ($p < .001$), lateral occipital cortex/middle temporal gyrus ($p < .001$), thalamus ($p < .001$), precentral gyrus ($p = .016$), frontal pole ($p = .028$), putamen/planum polare/insula ($p = .030$), and two clusters within the postcentral gyrus ($p = .01$ and .012, respectively). Qualitative examination of findings revealed two small clusters within the precuneus and Cerebellum I-IV that shared spatial overlap between the overall activation and frontal range of motion correlate analyses. The overlap in the Cerebellum I-IV was quantitatively supported with a liberal exploratory conjunction analysis (significant at z >

1.5, p < .05, but not at z >2.3), but the precuneus overlap was not statistically significant (z > 1.5, p > .05).

4. Discussion

The unique novelty of the present study was employing an MRI-compatible motion analysis system during a *multi*planar, lower-extremity fMRI leg press task that successfully quantified *single*-plane kinematic data for independent analyses with task-related brain activity collected concurrently. The task-associated neural activation during the leg press elicited distinct relationships with inter-subject variation in knee frontal plane mean ROM, but not knee sagittal plane ROM. Further, the present study was successful in overcoming traditional limitations of head motion artifact during task-based movement paradigms with fMRI. Specifically, usable neuroimaging data was obtained from 16 of the 17 participants, an improvement in usable data relative to a previous study using this paradigm (8 of 13 participants) (Grooms et al., 2019), plausibly due to the implementation of a robust statistical technique to remove head motion artifact (ICA-AROMA).

Overall, our whole-brain analyses demonstrated significant sensorimotor-related brain activity congruent with previous literature (e.g., pre and post central gyri) (Grooms et al., 2019). Our results further indicated that frontal plane ROM was distinctly associated with bidirectional activation in regions important for cognition (e.g., middle frontal gyrus, posterior cingulate cortex,), sensorimotor control (e.g., cerebellum, precentral gyrus) and sensorimotor integration (e.g., precuneus, postcentral gyrus). Previous studies have shown associations in neural activity measured during fMRI using extrinsic measures of kinematics of upper extremity movements of hands or arms (Haar et al., 2017; Widmer et al., 2017). The present study supports previous work demonstrating that various lower-extremity multi-joint movements during fMRI elicits distinct neural activity (Kapreli et al., 2007), and makes a unique contribution by isolating single-plane neural correlates of knee-joint kinematic data during a multi-joint movement.

Compared to traditional biomechanics testing for aberrant movements associated with high ACL injury risk biomechanics (e.g., drop vertical jump), the range of motion in the current study was smaller in both the frontal (2.5° vs ~8°) and sagittal planes (11.4° vs ~90°) (Hewett et al., 2015). This is plausibly due to traditional testing studies using more dynamic, unconstrained closed kinetic chain movements which could accentuate biomechanical deficiencies (drop vertical jump at participants' pace relative to the present, controlled leg press task) while movements during fMRI were restrictive to limit head motion. Despite differences in task constraints, the present study demonstrated that subtle variations in mean frontal ROM—during a paced movement with small kinematic variability (SD = 1.2°)—were distinctly associated with a bidirectional BOLD response in various regions important for attention, sensorimotor control, and sensorimotor integration (Figure 5), whereas no similar relationships were observed for brain activity and sagittal plane ROM. Increased frontal plane knee ROM, specifically knee valgus (out-of-plane) has been used as a marker of dynamic knee neuromuscular control due to its association with future primary and secondary ACL injury risk (Dingenen et al., 2015; Hewett et al., 2005; Paterno et al., 2010). The current results support the potential utility of knee frontal plane control

as an indicator of aberrant neural control of the lower extremity due to relationships with activity throughout numerous brain regions.

A potential contributor to the differences in relationships observed for the frontal relative to sagittal plane may be due to the available sagittal plane range of motion being greater compared to frontal plane motion ($>90°$ compared to $\sim15°$). As such, the volume of motion required to elicit comparable sagittal and frontal plane responses would require higher relative sagittal motion. A few degrees of frontal motion may differentially affect neural activity when compared to sagittal plane (Dai et al., 2001), as $2.5°$ in frontal plane represents 31% of available potential motion but 11.4 degrees in sagittal plane is only 13% of available motion (Hewett et al., 2005). As such, sagittal plane variation at the knee is more 'normal' to common multi-joint motion relative to frontal plane motion (i.e., in-plane versus out-of-plane). The absence of neural correlates for sagittal plane motion may potentially require a larger ROM to identify distinct relationships with brain activity and warrants future investigation.

Emerging evidence further indicates that subjects exhibiting high knee abduction moments (poor control of frontal plane ROM), a common ACL injury-risk indicator (Hewett et al., 2005), have distinct sensorimotor-related neural correlates as measured by electrocortical activity and resting-state functional connectivity (Bonnette et al., 2020; Diekfuss, Grooms, Bonnette, et al., 2020). As these studies measured brain activation in the absence of concurrent movement (i.e., at rest) or using EEG, the present data supplements these findings by utilizing a task-based, active knee motor control fMRI paradigm while quantifying associated biomechanics. With respect to lower extremity movement measurement methodologies concurrent to fMRI, prior studies have generally relied on inclinometers (Doolittle et al., 2020) or MRI-compatible accelerometers (Chung et al., 2011; Kim et al., 2013) for biomechanical-related performance outcome data. However, inclinometers are generally limited to single-plane measurements, and accelerometers are prone to 'drift bias' and require extensive calibration to achieve high quality data (Ghanbari & Yazdanpanah, 2015; Liu & Pang, 2001; Mazilu et al., 2011). The present study methods overcome previous performance-related limitations by employing an MRI-compatible system that was validated to a traditional 'gold standard', multi-camera 3D motion analysis system for the precise quantification of single-plane kinematic data during multiplanar motion. However, future research is needed to directly compare performance outcomes between the various methodologies, as well as for relative ease of implementation and feasibility for use with other integrated systems aiming to quantify multiplanar lower extremity motion during fMRI.

The methodologies from the current study can be extended to identify joint specific neural correlates for multi-joint movement coordination associated with various CNS pathologies affecting the lower extremity. Though future research is needed, this study provides preliminary data that may support the development of novel therapeutics aiming to supplement current, movement-based treatments for musculoskeletal injury prevention and rehabilitation using adjunctive, neural-targeted techniques (e.g., feedback and instruction to alter movement and brain activity) (Diekfuss, Bonnette, Hogg, et al., 2020; Gokeler et al., 2019).

Though this study was successful at achieving our aims, it is not without its limitations. First, the camera position and its field of view limits the range of motion that can be reliably measured when compared to traditional multi camera motion capture systems; however this is still a considerable advancement to previously metronome-paced paradigm that assume movement homogeneity across trial blocks and similarity between subjects. Second, while we were successful in isolating knee joint kinematics during our leg press task, a multi-camera MRI-compatible motion analysis system would be superior to have also identified the kinematics of the ankle and hip. Third, we did not quantify kinetics during the leg press task or standardize forces with the same level of biomechanical precision as kinematics (e.g., using a MRI-compatible load cell). Though force quantification was outside the scope of the present study aims, we recognize that intra- and inter-subject variability in force applied during the leg press may overlap, or be distinct, from the kinematic correlates identified. We emphasize future research employ the present methods with MRI-compatible force-quantification technologies to isolate the distinct kinematic and kinetic sensory contributions for brain activity, particularly in sensorimotor brain regions that may be important for sensing muscle length, joint position, etc. Finally, we did not quantify biomechanics of the leg contralateral to the moving leg to assess relative stabilization of the lower body during the fMRI paradigm. However, the contralateral leg was in full extension and likely required minimal activity as numerous physical restraints to the upper and mid torso were assistive to body stabilization. Nevertheless, future research should consider including measurements of neuromuscular activity (e.g., MRI-compatible electromyography) to confirm the relative amount of lower extremity activation in both the active and resting leg. Despite these limitations, the study demonstrates that single-joint kinematics during lower extremity, multi-joint movements elicit distinct neural correlates. Methodologies demonstrated in this study can be extended in future work and be applied to a broad scope of research questions regarding the role of lower extremity kinematics on brain activity for musculoskeletal-related injury and/or pathology.

5. Conclusion

The present study utilized an MRI-compatible 3D motion analysis system and identified distinct neural correlates of frontal plane ROM during a leg press task (out-of-plane), with greater knee frontal plane ROM eliciting significant, bidirectional relationships with brain activity in various regions important for attention, sensorimotor control, and sensorimotor integration. However, no distinct neural correlates of sagittal plane ROM during the leg press task were identified (in-plane motion). These data demonstrate the potential for the present methods to quantity and isolate the unique neural correlates of in- and out of plane knee biomechanics concurrent with fMRI, providing potentially tangible neural targets for adjunctive brain-based therapies theorized to promote injury-resistant movement (Armijo-Olivo, 2018; Diekfuss, Bonnette, Hogg, et al., 2020; Diekfuss, Grooms, Hogg, et al., 2020; Diekfuss, Hogg, Grooms, et al., 2020; Silfies et al., 2017).

Acknowledgement

Bibliography

Abram SGF, Price AJ, Judge A, & Beard DJ (2020). Anterior cruciate ligament (ACL) reconstruction and meniscal repair rates have both increased in the past 20 years in England: Hospital statistics from 1997 to 2017. British Journal of Sports Medicine, 54(5), 286–291. 10.1136/bjsports-2018-100195 [PubMed: 30661013]

Anand M, Diekfuss JA, Bonnette S, Hurn M, Short I, Grooms D, & Myer GD (2020). Validity of MRI-compatible motion capture system for use with lower extremity neuroimaging paradigms. International Journal of Sports Physical Therapy, 6. 10.26603/ijspt20200936

Anand M, Diekfuss JA, Slutsky-ganesh AB, Bonnette S, Grooms DR, & Myer GD (2020). SoftwareX Graphical interface for automated management of motion artifact within fMRI acquisitions : INFOBAR. SoftwareX, 12, 100598. 10.1016/j.softx.2020.100598 [PubMed: 33447655]

Andersson JLR, Jenkinson M, & Smith S. (2010a). Non-linear registration, aka spatial normalization (FMRIB technical report TR07JA2). June.

Andersson JLR, Jenkinson M, & Smith S. (2010b). Non-linear optimisation FMRIB Technial Report TR07JA1. June, 1–6. http://fsl.fmrib.ox.ac.uk/analysis/techrep/tr07ja1/tr07ja1.pdf

Armijo-Olivo S. (2018). A new paradigm shift in musculoskeletal rehabilitation: Why we should exercise the brain?Brazilian Journal of Physical Therapy, 22(2), 95–96. 10.1016/j.bjpt.2017.12.001 [PubMed: 29254876]

Bonnette S, Diekfuss JA, Grooms DR, Kiefer AW, Riley MA, Riehm C, Moore C, Barber Foss KD, Dicesare CA, Baumeister J, & Myer GD (2020). Electrocortical dynamics differentiate athletes exhibiting low-and high-ACL injury risk biomechanics. Psychhophysiology, June 2019, 15700. 10.1111/itor.12468

Chung SC, Kim HS, Yang JW, Lee SJ, Choi MH, Kim JH, Yeon HW, Park JY, Yi JH, & Tack GR (2011). A simple 5-DoF MR-compatible motion signal measurement system. Behavior Research Methods, 43(3), 897–901. 10.3758/s13428-011-0082-z [PubMed: 21487903]

Criss CR, Onate JA, & Grooms DR (2020). Neural activity for hip-knee control in those with anterior cruciate ligament reconstruction: A task-based functional connectivity analysis. Neuroscience Letters, 730, 134985. 10.1016/j.neulet.2020.134985 [PubMed: 32380143]

Dai TH, Liu JZ, Saghal V, Brown RW, & Yue GH (2001). Relationship between muscle output and functional MRI-measured brain activation. Experimental Brain Research, 140(3), 290–300. 10.1007/s002210100815 [PubMed: 11681304]

Diekfuss JA, Bonnette S, Hogg JA, Riehm C, Grooms DR, Singh H, Anand M, Slutsky-Ganesh AB, Wilkerson GB, & Myer GD (2020). Practical Training Strategies to Apply Neuro-Mechanistic Motor Learning Principles to Facilitate Adaptations Towards Injury-Resistant Movement in Youth. Journal of Science in Sport and Exercise. 10.1007/s42978-020-00083-0

Diekfuss JA, Grooms DR, Bonnette S, DiCesare CA, Thomas S, MacPherson RP, Ellis JD, Kiefer AW, Riley MA, Schneider DK, Gadd B, Kitchen K, Barber Foss KD, Dudley JA, Yuan W, & Myer GD (2020). Real- time biofeedback integrated into neuromuscular training reduces high-risk knee biomechanics and increases functional brain connectivity: A preliminary longitudinal investigation. Psychophysiology, 57(5), 2325967119S0002. 10.1111/psyp.13545

Diekfuss JA, Grooms DR, Hogg JA, Singh H, Slutsky-Ganresh AB, Bonnette S, Chris R, Anand M, Nissen KS, Wilkerson GB, & Myer GD (2020). Targeted application of motor learning theory to leverage youth neuroplasticity for enhanced injury-resistance and exercise performance: OPTIMAL PREP. Journal of Science in Sport and Exercise. 10.1007/s42978-020-00085-y

Diekfuss JA, Grooms DR, Nissen KS, Schneider DK, Foss KDB, Thomas S, Bonnette S, Dudley JA, Yuan W, Reddington DL, Ellis JD, Leach J, Gordon M, Lindsey C, Rushford K, Shafer C, & Myer GD (2019). Alterations in knee sensorimotor brain functional connectivity contributes to ACL injury in male high-school football players: a prospective neuroimaging analysis. Brazilian Journal of Physical Therapy. 10.1016/j.bjpt.2019.07.004

Diekfuss JA, Grooms DR, Yuan W, Dudley J, Barber Foss KD, Thomas S, Ellis JD, Schneider DK, Leach J, Bonnette S, & Myer GD (2019). Does brain functional connectivity contribute to musculoskeletal injury? A preliminary prospective analysis of a neural biomarker of ACL injury risk. Journal of Science and Medicine in Sport, 22(2), 169–174. 10.1016/j.jsams.2018.07.004 [PubMed: 30017465]

Diekfuss JA, Hogg JA, Grooms DR, Slutsky-Ganesh AB, Singh H, Bonnette S, Anand M, Wilkerson GB, & Myer GD (2020). Can We Capitalize on Central Nervous System Plasticity in Young Athletes to Inoculate Against Injury? Journal of Science in Sport and Exercise, 10.1007/s42978-020-00080-3

Dingenen B, Malfait B, Nijs S, Peers KHE, Vereecken S, Verschueren SMP, & Staes FF (2015). Can two-dimensional video analysis during single-leg drop vertical jumps help identify non-contact knee injury risk? A one-year prospective study. Clinical Biomechanics, 30(8), 781–787. 10.1016/j.clinbiomech.2015.06.013 [PubMed: 26144662]

Dobkin BH, Firestine A, West M, Saremi K, & Woods R. (2004). Ankle dorsiflexion as an fMRI paradigm to assay motor control for walking during rehabilitation. NeuroImage, 23(1), 370–381. 10.1016/j.neuroimage.2004.06.008 [PubMed: 15325385]

Doolittle JD, Downey RJ, Imperatore JP, Dowdle LT, Lench DH, McLeod J, McCalley DM, Gregory CM, & Hanlon CA (2020). Evaluating a novel MR-compatible foot pedal device for unipedal and bipedal motion: Test–retest reliability of evoked brain activity. Human Brain Mapping, September, 1–11. 10.1002/hbm.25209

Edwards AE, Guven O, Furman MD, Arshad Q, & Bronstein AM (2018). Electroencephalographic Correlates of Continuous Postural Tasks of Increasing Difficulty. Neuroscience, 395, 35–48. 10.1016/j.neuroscience.2018.10.040 [PubMed: 30391529]

Fukuyama H, Ouchi Y, Matsuzaki S, Nagahama Y, Yamauchi H, Ogawa M, Kimura J, & Shibasaki H. (1997). Brain functional activity during gait in normal subjects: a SPECT study. Neuroscience Letters, 228(3), 183–186. 10.1016/S0304-3940(97)00381-9 [PubMed: 9218638]

Gebel A, Lehmann T, & Granacher U. (2020). Balance task difficulty affects postural sway and cortical activity in healthy adolescents. Experimental Brain Research, 238(5), 1323–1333. 10.1007/s00221-020-05810-1 [PubMed: 32328673]

Ghanbari M, & Yazdanpanah MJ (2015). Delay Compensation of Tilt Sensors Based on MEMS Accelerometer Using Data Fusion Technique. IEEE Sensors Journal, 15(3), 1959–1966. 10.1109/JSEN.2014.2366874

Gokeler A, Neuhaus D, Benjaminse A, Grooms DR, & Baumeister J. (2019). Principles of motor learning to support neuroplasticity after ACL injury: Implications for optimizing performance and reducing risk of second ACL injury. Sports Medicine, 49(6), 853–865. 10.1007/s40279-019-01058-0 [PubMed: 30719683]

Griffanti L, Salimi-Khorshidi G, Beckmann CF, Auerbach EJ, Douaud G, Sexton CE, Zsoldos E, Ebmeier KP, Filippini N, Mackay CE, Moeller S, Xu J, Yacoub E, Baselli G, Ugurbil K, Miller KL, & Smith SM (2014). ICA-based artefact removal and accelerated fMRI acquisition for improved resting state network imaging. NeuroImage, 95, 232–247. 10.1016/j.neuroimage.2014.03.034 [PubMed: 24657355]

Grood ES, & Suntay WJ (1983). A joint coordinate system for the clinical description of three-dimensional motions: application to the knee. Journal of Biomechanical Engineering, 105(2), 136–144. http://www.ncbi.nlm.nih.gov/pubmed/6865355 [PubMed: 6865355]

Grooms DR, Diekfuss JA, Ellis JD, Yuan W, Dudley J, Foss KDB, Thomas S, Altaye M, Haas L, Williams B, Lanier JM, Bridgewater K, & Myer GD (2019). A novel approach to evaluate brain activation for lower extremity motor control. Journal of Neuroimaging, 29(5), 580–588. 10.1111/jon.12645 [PubMed: 31270890]

Grooms DR, Kiefer AW, Riley MA, Ellis JD, Thomas S, Kitchen K, DiCesare CA, Bonnette S, Gadd B, Barber Foss KD, Yuan W, Silva P, Galloway R, Diekfuss JA, Leach J, Berz K, & Myer GD (2018). Brain-behavior mechanisms for the transfer of neuromuscular training adaptions to simulated sport: Initial findings from the train the brain project. Journal of Sport Rehabilitation, 27(5), 1–5. 10.1123/jsr.2017-0241

Grooms DR, Page SJ, Nichols-Larsen DS, Chaudhari AMW, White SE, & Onate JA (2017). Neuroplasticity associated with anterior cruciate ligament reconstruction. Journal of Orthopaedic and Sports Physical Therapy, 47(3), 180–189. 10.2519/jospt.2017.7003

Grooms DR, Page SJ, & Onate JA (2015). Brain activation for knee movement measured days before second anterior cruciate ligament injury: Neuroimaging in musculoskeletal medicine. Journal of Athletic Training, 50(10), 1005–1010. 10.4085/1062-6050-50.10.02 [PubMed: 26509775]

Gwin JT, & Ferris DP (2012). An EEG-based study of discrete isometric and isotonic human lower limb muscle contractions. Journal of NeuroEngineering and Rehabilitation, 9(1), 1–11. 10.1186/1743-0003-9-35 [PubMed: 22244362]

Haar S, Donchin O, & Dinstein I. (2017). Individual movement variability magnitudes are explained by cortical neural variability. Journal of Neuroscience, 37(37), 9076–9085. 10.1523/JNEUROSCI.1650-17.2017 [PubMed: 28821678]

Havens KL, & Sigward SM (2015). Cutting mechanics: Relation to performance and anterior cruciate ligament injury risk. Medicine and Science in Sports and Exercise, 47(4), 818–824. 10.1249/MSS.0000000000000470 [PubMed: 25102291]

Hewett TE, Myer GD, Ford KR, Heidt RS, Colosimo AJ, McLean SG, Van Den Bogert AJ, Paterno MV, & Succop P. (2005). Biomechanical measures of neuromuscular control and valgus loading of the knee predict anterior cruciate ligament injury risk in female athletes: A prospective study. American Journal of Sports Medicine, 33(4), 492–501. 10.1177/0363546504269591

Hewett TE, Roewer B, Ford K, & Myer G. (2015). Multicenter trial of motion analysis for injury risk prediction: Lessons learned from prospective longitudinal large cohort combined biomechanical - epidemiological studies. Brazilian Journal of Physical Therapy, 19(5), 398–409. 10.1590/bjpt-rbf.2014.0121 [PubMed: 26537810]

Jaeger L, Marchal-Crespo L, Wolf P, Riener R, Kollias S, & Michels L. (2015). Test-retest reliability of fMRI experiments during robot-assisted active and passive stepping. Journal of NeuroEngineering and Rehabilitation, 12(1), 102. 10.1186/s12984-015-0097-2 [PubMed: 26577598]

Jaeger L, Marchal-Crespo L, Wolf P, Riener R, Michels L, & Kollias S. (2014). Brain activation associated with active and passive lower limb stepping. Frontiers in Human Neuroscience, 8. 10.3389/fnhum.2014.00828

Jenkinson M, Bannister P, Brady M, & Smith S. (2002). Improved Optimization for the Robust and Accurate Linear Registration and Motion Correction of Brain Images. NeuroImage, 17(2), 825–841. 10.1006/nimg.2002.1132 [PubMed: 12377157]

Jenkinson M, & Smith S. (2001). A global optimisation method for robust affine registration of brain images. Medical Image Analysis, 5(2), 143–156. 10.1016/S1361-8415(01)00036-6 [PubMed: 11516708]

Kapreli E, Athanasopoulos S, Gliatis J, Papathanasiou M, Peeters R, Strimpakos N, Van Hecke P, Gouliamos A, & Sunaert S. (2009). Anterior Cruciate Ligament Deficiency Causes Brain Plasticity. The American Journal of Sports Medicine, 37(12), 2419–2426. 10.1177/0363546509343201 [PubMed: 19940314]

Kapreli E, Athanasopoulos S, Papathanasiou M, Van Hecke P, Kelekis D, Peeters R, Strimpakos N, & Sunaert S. (2007). Lower Limb Sensorimotor Network: Issues of Somatotopy and Overlap. Cortex, 43(2), 219–232. 10.1016/S0010-9452(08)70477-5 [PubMed: 17405668]

Kim HS, Yeon HW, Choi MH, Yoon HJ, Kim HJ, Lee IH, Yi JH, & Chung SC (2013). Movement measurement systems for fMRI motion studies. Advanced Materials Research, 684, 473–476. 10.4028/www.scientific.net/AMR.684.473

la Fougère C, Zwergal A, Rominger A, Förster S, Fesl G, Dieterich M, Brandt T, Strupp M, Bartenstein P, & Jahn K. (2010). Real versus imagined locomotion: A [18F]-FDG PET-fMRI comparison. NeuroImage, 50(4), 1589–1598. 10.1016/j.neuroimage.2009.12.060 [PubMed: 20034578]

Liu HHS, & Pang GKH (2001). Accelerometer for mobile robot positioning. IEEE Transactions on Industry Applications, 37(3), 812–819. 10.1109/28.924763

Lohmander LS, Englund PM, Dahl LL, & Roos EM (2007). The Long-term Consequence of Anterior Cruciate Ligament and Meniscus Injuries. The American Journal of Sports Medicine, 35(10), 1756–1769. 10.1177/0363546507307396 [PubMed: 17761605]

MacIntosh BJ, Mraz R, Baker N, Tam F, Staines WR, & Graham SJ (2004). Optimizing the experimental design for ankle dorsiflexion fMRI. NeuroImage, 22(4), 1619–1627. 10.1016/j.neuroimage.2004.03.035 [PubMed: 15275918]

Malcolm BR, Foxe JJ, Butler JS, & De Sanctis P. (2015). The aging brain shows less flexible reallocation of cognitive resources during dual-task walking: A mobile brain/body

imaging (MoBI) study. NeuroImage, 117, 230–242. 10.1016/j.neuroimage.2015.05.028 [PubMed: 25988225]

Marchal-Crespo L, Michels L, Jaeger L, López-Olóriz J, & Riener R. (2017). Effect of Error Augmentation on Brain Activation and Motor Learning of a Complex Locomotor Task. Frontiers in Neuroscience, 11. 10.3389/fnins.2017.00526

Mazilu MT, Faranesh AZ, Derbyshire JA, Lederman RJ, & Hansen MS (2011). Low-Cost MRI Compatible Interface Device for Interactive Scan Plane Control. Proceedings of the 19th Scientific Meeting of ISMRM, Montreal, Quebec, Canada, 19, 3752.

Mehta JP, Verber MD, Wieser JA, Schmit BD, & Schindler-Ivens SM (2009). A novel technique for examining human brain activity associated with pedaling using fMRI. Journal of Neuroscience Methods, 179, 230–239. 10.1016/j.jneumeth.2009.01.029 [PubMed: 19428532]

Needle AR, Lepley AS, & Grooms DR (2017). Central Nervous System Adaptation After Ligamentous Injury: a Summary of Theories, Evidence, and Clinical Interpretation. Sports Medicine, 47(7), 1271–1288. 10.1007/s40279-016-0666-y [PubMed: 28005191]

Neto T, Sayer T, Theisen D, & Mierau A. (2019). Functional Brain Plasticity Associated with ACL Injury: A Scoping Review of Current Evidence. Neural Plasticity, 2019, 1–17. 10.1155/2019/3480512

Oliveira AS, Schlink BR, David Hairston W, König P, & Ferris DP (2017). A channel rejection method for attenuating motion-related artifacts in EEG recordings during walking. Frontiers in Neuroscience, 11(APR), 1–17. 10.3389/fnins.2017.00225 [PubMed: 28154520]

Oliveira AS, Schlink BR, Hairston WD, König P, & Ferris DP (2016). Induction and separation of motion artifacts in EEG data using a mobile phantom head device. Journal of Neural Engineering, 13(3), 036014. 10.1088/1741-2560/13/3/036014 [PubMed: 27137818]

Paterno MV, Schmitt LC, Ford KR, Rauh MJ, Myer GD, Huang B, & Hewett TE (2010). Biomechanical measures during landing and postural stability predict second anterior cruciate ligament injury after anterior cruciate ligament reconstruction and return to sport. The American Journal of Sports Medicine, 38(10), 1968–1978. 10.1177/0363546510376053 [PubMed: 20702858]

Pelletier R, Higgins J, & Bourbonnais D. (2015). Is neuroplasticity in the central nervous system the missing link to our understanding of chronic musculoskeletal disorders? BMC Musculoskeletal Disorders, 16(1), 1–13. 10.1186/s12891-015-0480-y [PubMed: 25637090]

Peterson SM, & Ferris DP (2018). Differentiation in Theta and Beta Electrocortical Activity between Visual and Physical Perturbations to Walking and Standing Balance. Eneuro, 5(4), ENEURO.0207-18.2018. 10.1523/ENEURO.0207-18.2018

Pruim RHR, Mennes M, van Rooij D, Llera A, Buitelaar JK, & Beckmann CF (2015). ICA-AROMA: A robust ICA-based strategy for removing motion artifacts from fMRI data. NeuroImage, 112, 267–277. 10.1016/j.neuroimage.2015.02.064 [PubMed: 25770991]

Rummel C, Verma RK, Schöpf V, Abela E, Hauf M, Berruecos JFZ, & Wiest R. (2013). Time Course Based Artifact Identification for Independent Components of Resting-State fMRI. Frontiers in Human Neuroscience, 7(May), 1–8. 10.3389/fnhum.2013.00214 [PubMed: 23355817]

Seeber M, Scherer R, Wagner J, Solis-Escalante T, & Müller-Putz GR (2014). EEG beta suppression and low gamma modulation are different elements of human upright walking. Frontiers in Human Neuroscience, 8. 10.3389/fnhum.2014.00485

Seeber M, Scherer R, Wagner J, Solis-Escalante T, & Müller-Putz GR (2015). High and low gamma EEG oscillations in central sensorimotor areas are conversely modulated during the human gait cycle. NeuroImage, 112, 318–326. 10.1016/j.neuroimage.2015.03.045 [PubMed: 25818687]

Silfies SP, Vendemia JMC, Beattie PF, Stewart JC, & Jordon M. (2017). Changes in brain structure and activation may augment abnormal movement patterns: An emerging challenge in musculoskeletal rehabilitation. Pain Medicine, 18(11), 2051–2054. 10.1093/pm/pnx190 [PubMed: 29121336]

Smith SM (2002). Fast robust automated brain extraction. Human Brain Mapping, 17(3), 143–155. 10.1002/hbm.10062 [PubMed: 12391568]

Suzuki M, Miyai I, Ono T, & Kubota K. (2008). Activities in the frontal cortex and gait performance are modulated by preparation. An fNIRS study. NeuroImage, 39(2), 600–607. 10.1016/j.neuroimage.2007.08.044 [PubMed: 17950626]

Swanik C. "Buz." (2015). Brains and Sprains: The Brain's Role in Noncontact Anterior Cruciate Ligament Injuries. Journal of Athletic Training, 50(10), 1100–1102. 10.4085/1062-6050-50.10.08 [PubMed: 26340611]

Te M, Baptista AF, Chipchase LS, & Schabrun SM (2017). Primary Motor Cortex Organization Is Altered in Persistent Patellofemoral Pain. Pain Medicine, 18(11), 2224–2234. 10.1093/pm/pnx036 [PubMed: 28340134]

Tohka J, Foerde K, Aron AR, Tom SM, Toga AW, & Poldrack RA (2008). Automatic independent component labeling for artifact removal in fMRI. NeuroImage, 39(3), 1227–1245. 10.1016/j.neuroimage.2007.10.013 [PubMed: 18042495]

Umberger BR, & Caldwell GE (2014). Research Methods in Biomechanics: Musculoskeletal Modeling (Issue November 2013).

Vitorio R, Stuart S, Rochester L, Alcock L, & Pantall A. (2017). fNIRS response during walking — Artefact or cortical activity? A systematic review. Neuroscience & Biobehavioral Reviews, 83, 160–172. 10.1016/j.neubiorev.2017.10.002 [PubMed: 29017917]

Wagner J, Martinez-Cancino R, Delorme A, Makeig S, Solis-Escalante T, Neuper C, & Mueller-Putz G. (2019). High-density EEG mobile brain/body imaging data recorded during a challenging auditory gait pacing task. Scientific Data, 6(1), 211. 10.1038/s41597-019-0223-2 [PubMed: 31624252]

Weinhandl JT, Armstrong BSR, Kusik TP, Barrows RT, & O'Connor KM (2010). Validation of a single camera three-dimensional motion tracking system. Journal of Biomechanics, 43(7), 1437–1440. 10.1016/j.jbiomech.2009.12.025 [PubMed: 20207358]

Widmer M, Stulz S, Luft AR, & Lutz K. (2017). Elderly adults show higher ventral striatal activation in response to motor performance related rewards than young adults. Neuroscience Letters, 661(September), 18–22. 10.1016/j.neulet.2017.09.038 [PubMed: 28939388]

Woolrich MW, Ripley BD, Brady M, & Smith SM (2001). Temporal autocorrelation in univariate linear modeling of FMRI data. NeuroImage, 14(6), 1370–1386. 10.1006/nimg.2001.0931 [PubMed: 11707093]

Highlights

1. Brain activity was measured using fMRI during a leg press task

2. An MRI-compatible motion capture system concurrently collected knee biomechanics

3. Increased out-of-plane (frontal) angle associated with altered brain activity

4. No similar in-plane (sagittal) neural correlates were identified

Figure 1.
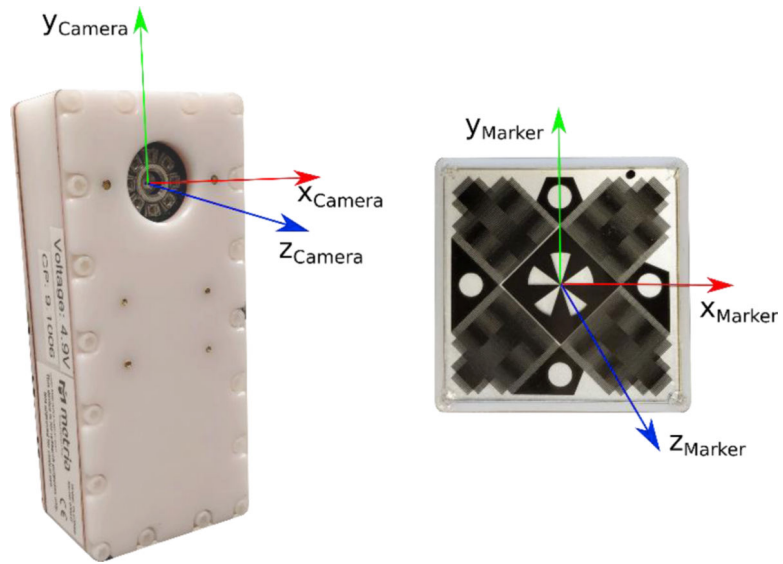A subject in the MRI with the MPT markers performing the unilateral leg press task.

Figure 2.
(a) MPT camera with its axis overlay. (b) MPT compatible marker showing the Moiré pattern and axis overlay.
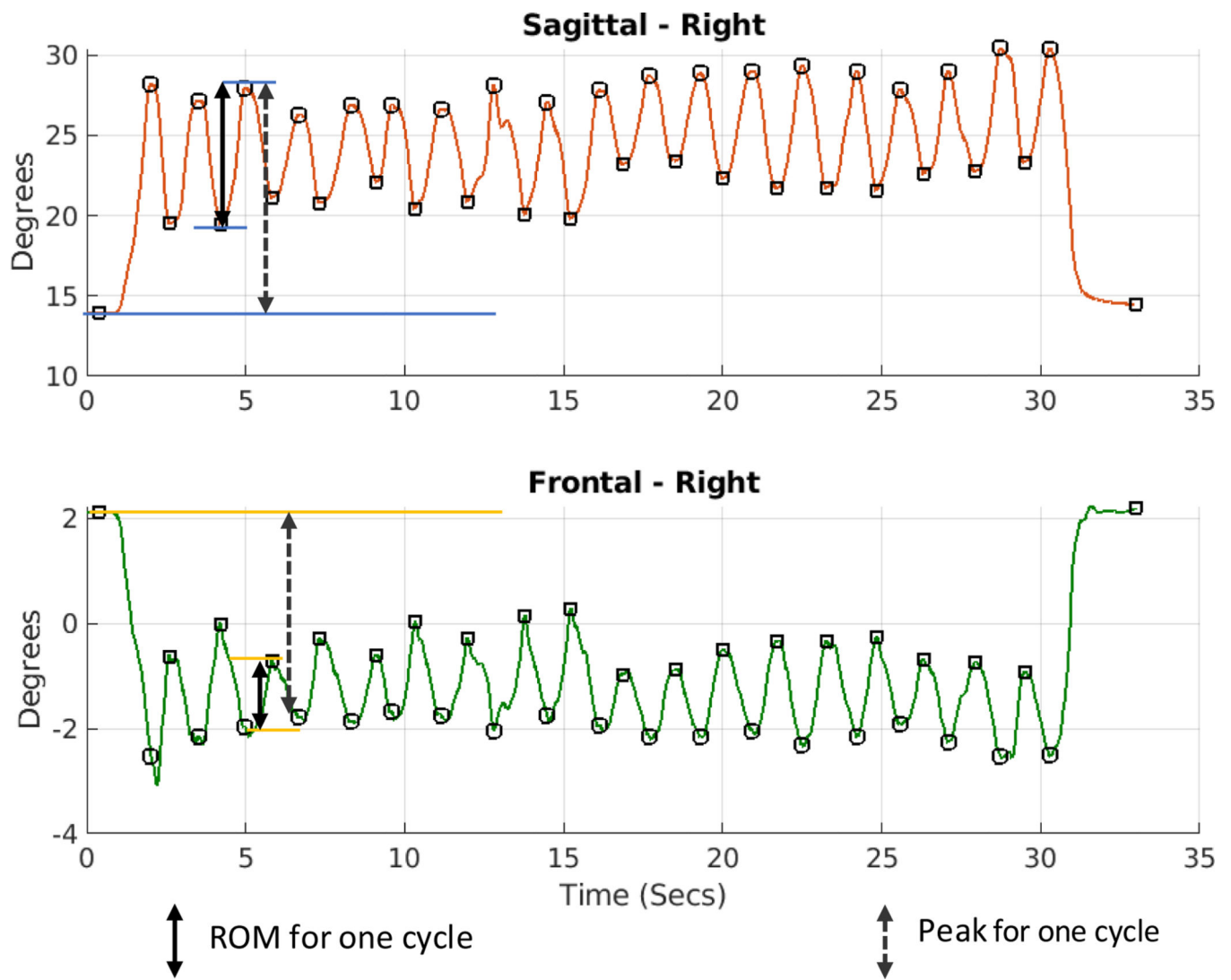
Fig. 3.
Knee sagittal and frontal plane angles of a representative subject during a movement block.
Calculation of range of motion (ROM) for one cycle within the block is shown with the
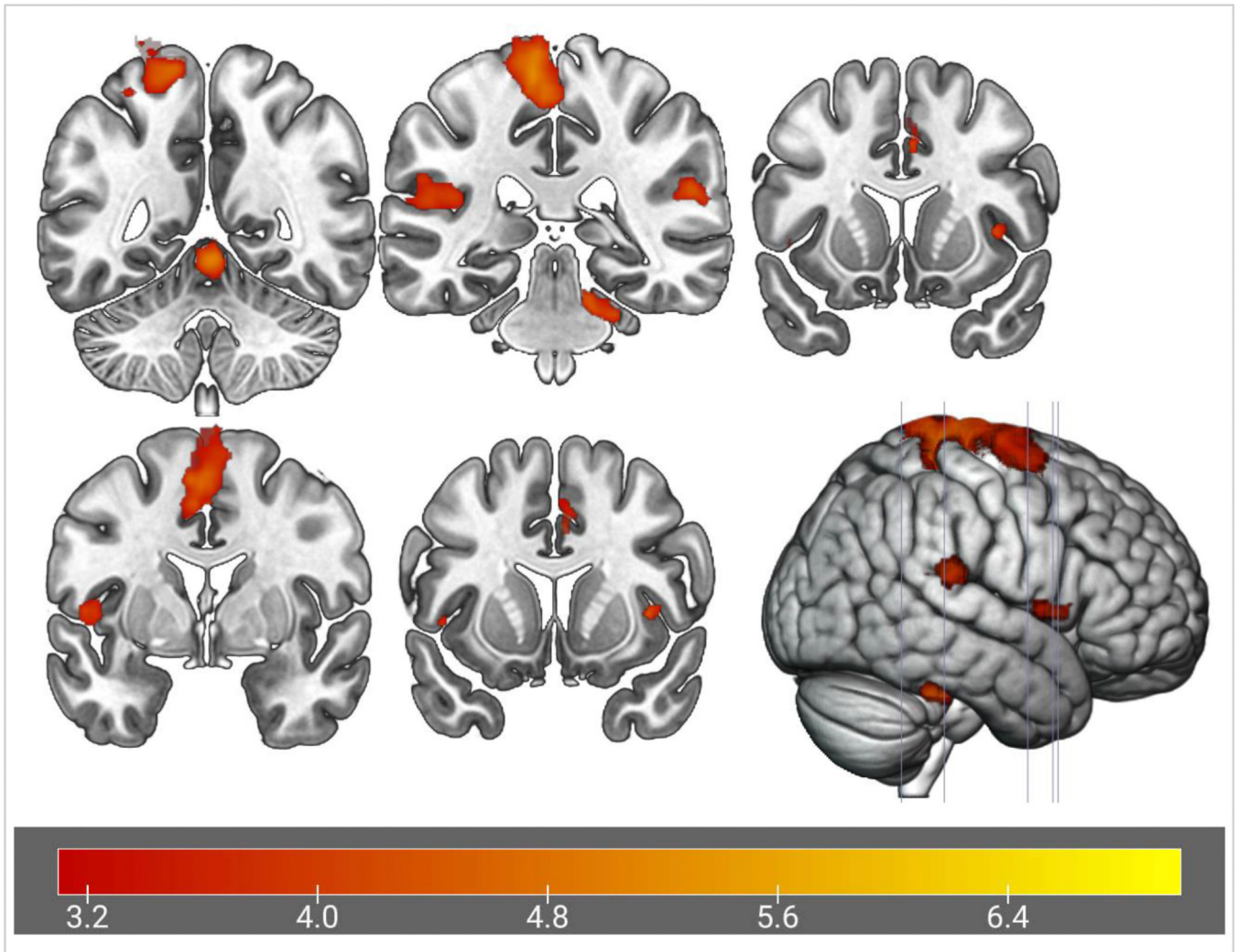overlaid arrows.

Figure 4.
Z-score map for overall brain activation during task performance. The cluster-wise threshold was set at Z > 3.1, p < .05.

Figure 5.
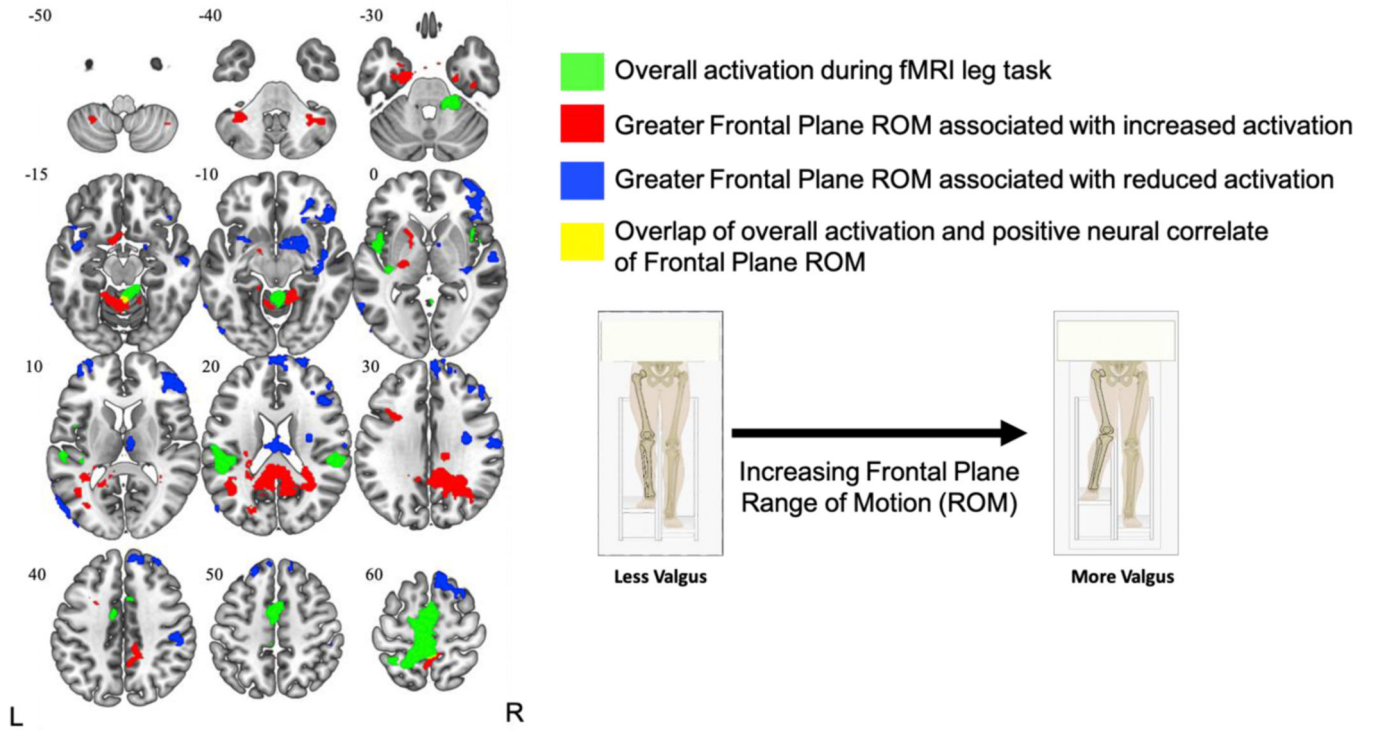Brain activation during the fMRI leg task (green) and neural correlates of Frontal Plane
Range of Motion (positive = red, negative = blue) shown in the axial view with Z-coordinate
slices. Small yellow clusters in the Precuneus (slice: −15) and Cerebellum I-IV (slice:
60) represent spatial areas of overlap between overall activation and positive correlates of
Frontal Range of Motion. L = left, R = right.

Table 1.

Significant clusters and peaks of activation during the leg press task, relative to rest

	Region$_{cluster}$	Primary Hemisphere	Size$_{cluster}$ (mm³)	Region$_{peak}$	Zmax$_{peak}$	MNI Coordinates X, Y, Z$_{peak}$	p-value
Overall Brain Activation During Leg Press Task	Supplementary Motor Cortex, Precentral Gyrus, Postcentral Gyrus	L	4269	Precentral gyrus	5.77	−12, −12, 62	<.001
	Parietal Operculum, Planum Temporale	L	722	Parietal operculum	4.22	−40, −32, 18	<.001
	Parietal Operculum, Planum Temporale	R	251	Planum temporale	4.57	54, −34, 20	.001
	Insula, Central Operculum	L	161	Central Operculum	4.19	−48, 0, 4	.013
	Insula, Central Operculum	R	131	Insula	4.37	38, 10, 2	.034
	Cerebellum I-IV	R	712	Cerebellum I-IV	5.19	2, −50, −8	<.001

Table 2.

Significant clusters and peaks of activation of correlates with frontal plane range of motion, relative to rest

		Positive Associations					
	Region$_{cluster}$	Primary Hemisphere	Size$_{cluster}$ (mm^3)	Region$_{peak}$	Zmax$_{peak}$	MNI Coordinates X, Y, Z$_{peak}$	p-value
Neural Correlates of Frontal Range of Motion	Posterior Cingulate Cortex, Precuneus	R	3280	Posterior cingulate cortex	8.31	−4, −44, 20	<.001
	Precuneus	L	125	Precuneus	4.4	−4, −54, 60	.040
	Cerebellum V, Cerebellum I-IV	L	383	Cerebellum V	5.46	−6, −56, −10	<.001
	Parahippocampus, Temporal Fusiform Gyrus	L	364	Parahippocampus	4.88	−32, −14, −32	<.001
	Parahippocampus, Temporal Fusiform Gyrus	R	180	Temporal fusiform gyrus	4.46	40, −12, −26	.007
	Pallidum	L	271	Pallidum	4.96	−16, 6, 6	<.001
	Cerebellum VIIIa, Cerebellum VIIIb	L	192	Cerebellum VIIIa	4.67	−28, −48, −48	.005
	Cerebellum Crus I	R	180	Cerebellum Crus I	5.75	40, −54, −36	.008
	Middle Frontal Gyrus	L	125	Middle Frontal Gyrus	5.31	−38, 16, 30	.022
	Negative Associations						
	Region$_{cluster}$	Primary Hemisphere	Size$_{cluster}$ (mm^3)	Region$_{peak}$	Zmax$_{peak}$	MNI Coordinates X, Y, Z$_{peak}$	p-value
	Frontal Pole, Superior Frontal Gyrus	R	3132	Frontal Pole	7.63	4, 58, 30	<.001
	Planum Polare, Insula, Pallidum	R	827	Planum Polare	6.1	44, −4, −12	<.001
	Lateral Occipital Cortex, Middle Temporal Gyrus	L	539	Lateral Occipital Cortex	5.95	−52, −80, −2	<.001
	Thalamus	R	292	Thalamus	6.52	4, −16, 12	<.001
	Postcentral Gyrus	R	163	Postcentral Gyrus	6.52	48, −24. 44	.011
	Postcentral Gyrus	R	163	Postcentral Gyrus	4.21	62, −12, 30	.012
	Precentral Gyrus	R	153	Precentral Gyrus	5.05	42, 4, 26	.016
	Frontal Pole	L	135	Frontal Pole	5.05	−38, 58, 8	.028
	Putamen, Planum Polare, Insula	L	133	Putamen	4.59	−22, 4, −10	.030